Available online at www.sciencedirect.com

ScienceDirect

Current Opinion in Electrochemistry

Review Article

Scalable fabrication of sheet-type electrodes for practical all-solid-state batteries employing sulfide solid electrolytes

Kyu Tae Kim, Tae Young Kwon and Yoon Seok Jung

Abstract

The limited safety and energy density of conventional lithium-ion batteries have triggered the research and development of all-solid-state Li or Li-ion batteries (ASLBs). Sulfide solid electrolytes possess the remarkable advantages combining high ionic conductivity and mechanical deformability that allows for simple cold-pressing based fabrication of the cells. For this reason, these electrolytes find promising application in practical ASLBs. However, the large gap between experimental laboratory research and practical applications poses a formidable challenge. Herein, recent studies on scalable fabrication strategies for ASLBs employing sulfide solid electrolytes are discussed. The critical factors for wet-slurry and dry-film fabrication methods are reviewed. Based on these results, recent developments in slurry-processing solvents, polymeric binders, and fabrication protocols are summarized. Finally, the advantages and disadvantages of the two fabrication protocols are summarized, along with prospects for future research.

Addresses

Department of Chemical and Biomolecular Engineering, Yonsei University, Seoul 03722, South Korea

Corresponding author: Jung, Yoon Seok (yoonsjung@yonsei.ac.kr)

Current Opinion in Electrochemistry 2022, **34**:101026

This review comes from a themed issue on **Energy Storage**

Edited by **Jang Wook Choi** and **Yan Yao**

For a complete overview see the Issue and the Editorial

Available online 19 April 2022

https://doi.org/10.1016/j.coelec.2022.101026

Introduction

High-energy lithium-ion batteries (LIBs) have revolutionized energy storage technologies and are currently considered indispensable power sources for portable electronic devices, electric vehicles, and grid-scale energy storage systems [1,2]. Although these advances are attributable to the development of optimal organic liquid electrolytes, safety concerns stemming from their flammability are unavoidable [3]. In this regard, all-solid-state Li or Li-ion batteries (ASLBs) employing non-flammable inorganic solid electrolytes (SEs) have attracted much attention as promising post-LIBs [4]. Furthermore, the solidification of electrolytes has a potential to stabilize next-generation high-capacity anodes such as Li metal and Si [5,6]. Stackable design of electrodes can also increase the system-level energy density of the batteries [7,8].

SEs are key components of ASLBs and are categorized into two types: polymer SEs and inorganic SEs. Polymer electrolytes are highly attractive because of their soft mechanical properties and processability at scale [9]. Gel polymer electrolytes, which are composed of polymers, Li salts, and plasticizers, show moderate Li^+ conductivities (typically <1 mS cm^{-1}) [10] but suffer from disadvantages observed in conventional liquid electrolytes, such as safety problems and swelling caused by electrolyte decomposition [11]. Although solid (or dry) polymer electrolytes, that are free of plasticizers, may show improved safety, their conductivities remain too low (typically $<10^{-4}$ S cm^{-1}) [10]. In contrast, state-of-the-art inorganic SEs, such as sulfides (e.g., $Li_{5.5}PS_{4.5}Cl_{1.5}$: [12]: 12 mS cm^{-1}), oxides (e.g., $Li_7La_3Zr_2O_{12}$ [13]: 0.1–1 mS cm^{-1}), halides (e.g., Li_3YCl_6 [14]: 0.51 mS cm^{-1}), and closo-borates (e.g., $0.7Li(CB_9H_{10})$-$0.3Li(CB_{11}H_{12})$ [15]: 6.7 mS cm^{-1}), show Li^+ conductivities comparable to or even superior to those of liquid electrolytes ($\sim$10 mS cm^{-1}) [3]. In particular, as sulfide SEs are mechanically sinterable by simple cold-pressing, their applications in the fabrication of ASLBs have been rigorously pursued [4,16].

However, there is still a large gap between laboratory research and the practical applications of ASLB technologies based on sulfide SEs. Concerns include chemical vulnerability to ambient air or organic solvents, detrimental interfacial electrochemical and electrochemo-mechanical effects, high cost and time-consuming production of SE materials, and high operational pressure for maintaining solid–solid contacts [4,17]. In particular, the poor chemical stability of sulfide SEs leads to degradation when they come into contact with organic solvents, which greatly restricts the wet-slurry fabrication protocol for large-format sheet-type electrodes and SE membranes [18–20]. The

representative restrictions are briefly summarized as follows. (1) Chemical degradation induced by organic solvents: with increasing polarity of the solvents, the chemical degradation of sulfide SEs becomes more prominent [18,19,21,22]. Accordingly, nonpolar or less polar solvents, such as toluene, xylene, and heptane, have been used, but they are highly volatile and result in poor distribution of the electrode components. To exacerbate, less polar solvents can also cause slight elution of the sulfide SEs during processing [23]. (2) Limited solvent−binder combinations due to "polarity mismatch": because of the poor compatibility with commonly used solvents, polymeric binder candidates are also limited to rubber-based binders (e.g., nitrile butadiene rubber (NBR) and butadiene rubber (BR)) that are soluble in low-polarity solvents [18,21]. Furthermore, this feature complicates the design of functional binders that can cope with the detrimental electrochemo-mechanical effects or the electrochemical degradation of polymeric binders. (3) Li^+ hindrance by insulating polymeric binders: in LIBs, binders are soaked in liquid electrolytes and thus become Li^+-conductive, while the binders in ASLBs remain Li^+-insulating [18]. Even with a small amount of binder (1−2 wt.%), the capacity of ASLB cells could decrease by a maximum of 30 mA h g^{-1} [18]. (4) Weak adhesion of less polar polymeric binders: it is widely accepted that polar groups in polymeric binders form strong interactions between the lone pair electrons in the polar functional groups and the unoccupied orbital of −H in the electrode active materials or current collectors [24]. The absence of highly polar functional groups in many polymeric binders for ASLBs complicates the fabrication of robust electrodes. (5) The general criteria for slurry-processing solvents, including volatility, toxicity, and ability to distribute components, have been overlooked. For example, *o*-xylene and *n*-heptane, which have been widely investigated for use in ASLB fabrication, are harmful and volatile, respectively. In this review, based on the aforementioned motivation and background, we discuss recent developments and perspectives in the scalable fabrication strategies for practical sulfide SE-based ASLBs.

Wet-slurry fabrication of ASLBs

Since the first report on pouch-type MoS_8/Li−Al ASLB cells was published in 2009 [25], many papers have documented a fundamental understanding and practical guidelines for wet-slurry fabrication methods for ASLBs [18,21,26−29]. Table 1 summarizes the solvents and binders for the wet-slurry fabrication of ASLB electrodes using sulfide SEs. In this section, the research history of solvents and polymeric binders for the wet-slurry fabrication of sulfide-based ASLBs is explained in detail.

Table 1

Solvents and binders used for wet-slurry fabrication of ASLB electrodes using sulfide SEs.

Active material	Solid electrolytes	Solvent	Binder	Ref
Mo_6S_8	$Li_{3.25}Ge_{0.25}P_{0.75}S_4$	Heptane	Polysiloxane	[25]
NCA801505	$80Li_2S−20P_2S_5$	Xylene	Nitrile butadiene rubber (NBR)	[26]
NCM111 Graphite	Li_3PS_4	Anisole	Styrene butadiene styrene (SBS)	[27]
NCM111		Heptane	Styrene ethylene butylene styrene copolymer (SEBS)	
NCM811	Li_3PS_4	*p*-xylene	NBR	[21]
NCM111	Li_3PS_4	*n*-decane	SEBS	[31]
NCM622 Graphite	Li_6PS_5Cl	Xylene	NBR	[18]
NCM111 Graphite	Li_3PS_4	Anisole	Poly(propylene carbonate) *Removed by heating	[22]
NCM111 Si	Li_3PS_4	Anisole	Poly(propylene carbonate) *Removed by heating	[43]
NCM622	Li_3PS_4	Toluene	Oppanol	[29]
NCM111	Li_3PS_4	Anisole Heptane	SBR SEBS	[33]
NCM711	Li_6PS_5Cl	*p*-xylene	Butadiene rubber (BR) SBS-COOH click binder	[44]
NCM711 NCM622	Li_6PS_5Cl	Dibormomethane	NBR NBR-Li(G3)TFSI	[19]
NCM711	Li_6PS_5Cl	Butyl butyrate	BR Poly(tert-butyl acrylate) (TBA) TBA-b-BR	[45]
NCM811	$Li_{10}GeP_2S_{12}$	Xylene	NBR Poly(ethylene oxide)-LiTFSI-Pyr_{14}TFSI	[46]

Table 1 (*continued*)

Active material	Solid electrolytes	Solvent	Binder	Ref
NCM711 Graphite	$Li_6PS_5Cl_{0.5}Br_{0.5}$	Dibormomethane + Hexyl butyrate	NBR NBR-LiTFSI	[34]
NCM711 Graphite	$Li_6PS_5Cl_{0.5}Br_{0.5}$	Benzyl acetate	NBR-poly(1,4-butylene adipate) NBR-poly(1,4-butylene adipate)-LiTFSI	[23]
NCM622	Li_3PS_4	*o*-xylene	Oppanol SBR Hydrogenated NBR	[42]
LCO Graphite	0.4LiI-0.6Li_4SnS_4 Li_6PS_5Cl	Methanol Ethanol	PVdF	[50]
LCO Si	Li_6PS_5Cl	Ethanol	PVdF	[55]
LCO Graphite	$Li_6PS_5Cl_{0.5}Br_{0.5}$	Ethanol	PVdF	[52]
NCM111	Li_6PS_5Cl	Ethanol	Ethyl cellulose	[39]
NCM811	Li_6PS_5Cl	Ethanol	Ethyl cellulose	[40]
NCM622 Graphite	Li_2S-P_2S_5	Tetrahydorfuran	NBR Polyvinylchloride (PVC)	[54]

Selection of solvents

In conventional LIBs, electrodes are fabricated using *N*-methyl-2-pyrrolidone (NMP) or water, which not only effectively distributes the components but also dissolves various polar polymeric binders, such as polyvinylidene fluoride (PVdF) and styrene-butadiene rubber (SBR)/sodium salt of carboxymethyl cellulose (CMC). However, highly polar solvents readily decompose sulfide SEs via nucleophilic attack. Lee et al. suggested selection strategies for processing solvents for sulfide SE-based electrodes [21]. Screening of a variety of solvents revealed that the polarity index of the solvent is the most critical factor affecting compatibility with sulfide SEs. In a similar context, Yamamoto et al. investigated the effects of solvent exposures toward sulfide SEs (Figure 1a) [22]. These results implied that the donor number (DN) of the solvent could be an indicator of the selection criteria. Recently, the degradation mechanism of tetra-Li_7SiPS_8 in protic and aprotic solvents has been investigated [30]. Magic angle spinning ^{31}P nuclear magnetic resonance (NMR) spectra revealed that nucleophilic attack of alcohol and water formed oxygen-substituted thioether and oxygen-substituted thiophosphates, respectively. In contrast, aprotic solvents with a DN < 15 kJ mol^{-1} dissolved the amorphous Li_3PS_4-type phase and led to the formation of various polysulfide species, which imparted color to the suspensions. Furthermore, the detrimental interphase was formed by complex behavior including the presence of residual solvent, solvent–particle interactions, and decomposition products, which further induced a decrease in the Li^+ conductivity, especially when the DN > 15 kJ mol^{-1}. Although the polarity index or DN can effectively predict the compatibility of each solvent with detailed mechanisms, these indicators are often unknown for less used solvents. Oh et al. reported simple strategies for selecting solvents based on the functional groups and steric hindrance effects (Figure 1b) [23]. While ethyl acetate possessing a polar ester group severely degraded sulfide SEs, benzyl acetate with the same ester group showed decent compatibility with sulfide SEs, which was attributed to the steric hindrance by the bulky benzyl group.

Besides the chemical compatibility of solvents with sulfide SEs, there are more requirements for the wet-slurry fabrication of practical sheet-type ASLB electrodes, including adequate volatility, ability to distribute components, and nontoxicity. Yamamoto et al. investigated the effects of vapor pressure on the microstructural morphology of the electrodes [31]. Figure 1c shows two electrode sheets fabricated using 1,2-dichloroethane (upper panel) and *n*-decane (lower panel). The electrode fabricated using volatile 1,2-dichloroethane (vapor pressure of 10.2 kPa at 298 K, boiling point of 83.47 °C) had a rough surface with some protrusions and delamination from the current collector. In contrast, the electrode fabricated using the less volatile *n*-decane (vapor pressure of 0.17 kPa at 298 K, boiling point of 174.1 °C) had a dense and smooth surface. The poor electrode properties observed when using volatile solvents are responsible for the high drying rate of the slurries, which provokes binder migration and weak adhesion [32]. The distribution of multiple components in the slurries is another important issue [28,33]. Chen et al. investigated the reaction distribution within ASLB electrodes prepared using different binder materials and solvents [33]. Two-dimensional (2D)-imaging X-ray absorption spectroscopy indicated that electrodes using SBR with anisole had a well-distributed morphology, while electrodes using styrene-ethylene-butylene-styrene (SEBS) with

Figure 1

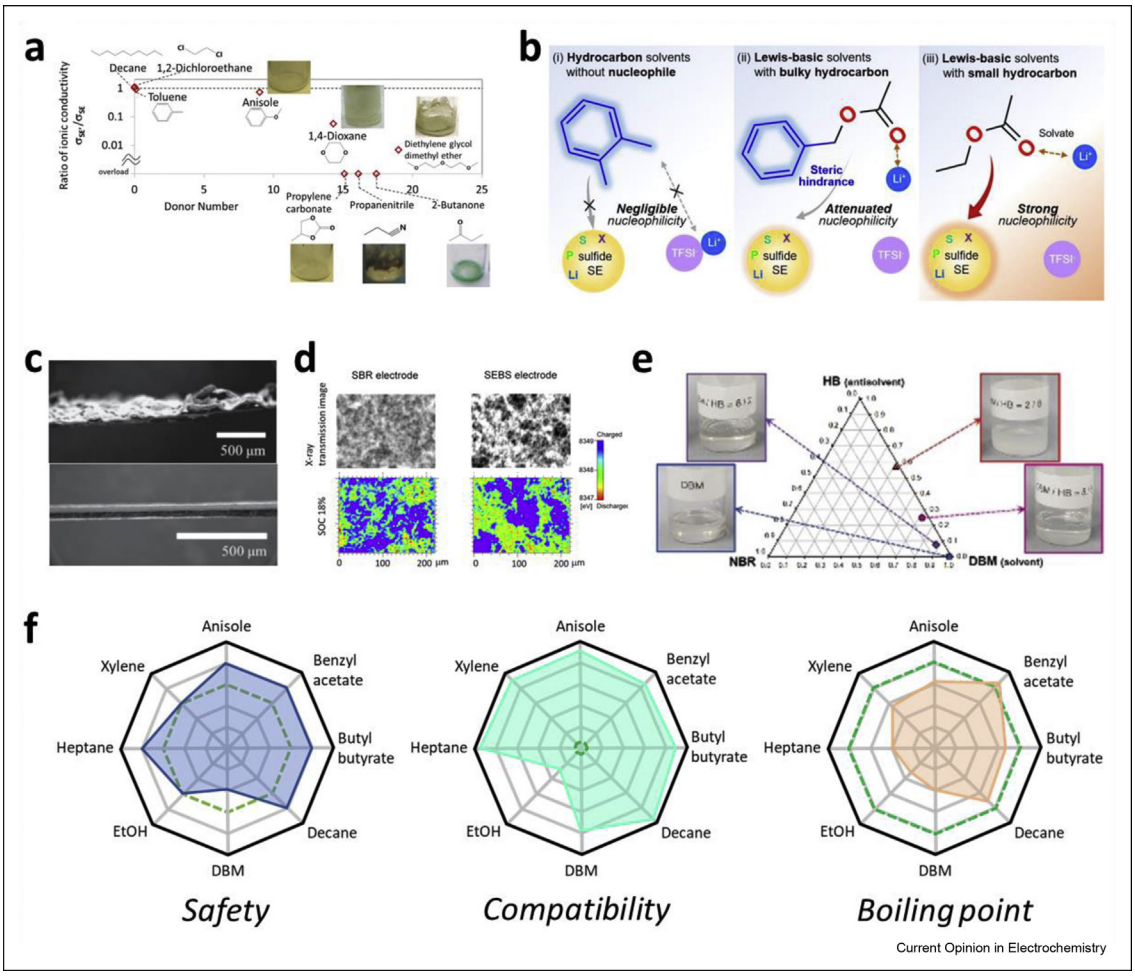

Selection criteria of slurry-processing solvents for sulfide SE-based ASLBs. (**a**) Ratio of ionic conductivity for solvent-exposed and pristine Li_3PS_4 as a function of the DN of the solvents. Reproduced with permission from Ref. [22], Copyright 2018, Nature Publishing Group. (**b**) Schematic of the reactivity with $Li_6PS_5Cl_{0.5}Br_{0.5}$ for (i) hydrocarbon solvents, (ii) Lewis-basic solvents with bulky hydrocarbons, and (iii) Lewis-basic solvents with small hydrocarbons. Reproduced with permission from Ref. [23], Copyright 2021, Wiley-VCH. (**c**) Cross-sectional SEM images of composite electrodes formed by coating the slurry using 1,2-dichloroethane (upper) and *n*-decane (lower). Reproduced with permission from Ref. [31], Copyright 2017, Ceramic Society of Japan. (**d**) X-ray transmission images and reacted area mapping results for 11% of SOC in the in-plane direction for the SBR electrode (left side) and SEBS electrode (right side). Reproduced with permission from Ref. [33], Copyright 2019, American Chemical Society. (**e**) Ternary diagram of the NBR-DBM-HB system and corresponding photographs. Reproduced with permission from Ref. [34], Copyright 2021, Wiley-VCH. (**f**) Spider plots comparing representative processing solvents for sulfide SEs. The dashed green lines in (f) indicate each level of the conventional processing solvent NMP.

heptane had an aggregated morphology (Figure 1d). Electrodes with better distribution exhibited superior electrochemical performance and diminished impedance. However, it is uncertain which of the following plays a more dominant role in the aforementioned phenomenon: the solvent, binder, or a solvent—binder combination. Kim et al. discovered that the introduction of the cosolvent dibromomethane (DBM)-hexyl butyrate (HB), where DBM and HB acted as the solvent and antisolvent for NBR, respectively, could control the distribution of polymeric binders [34]. As the volume fraction of anti-solvent HB was increased, the NBR solution became turbid (Figure 1e), indicating entanglement of the polymeric domains, which was confirmed by dynamic light scattering measurements. This aggregated feature of binders in the slurries using cosolvents resulted in less obstructed Li^+ contacts between cathode active materials (CAMs) and SEs in electrodes as compared to the case of electrodes fabricated using a single solvent DBM. Recently, Ruhl et al. reported an unexpected drop in the conductivity when Li_6PS_5Cl was exposed to toluene [35]. X-ray diffraction (XRD) and Raman spectroscopy results indicated that toluene-treated Li_6PS_5Cl retained its original structure. However, scanning electron microscopy (SEM) observations clearly showed that toluene-treated Li_6PS_5Cl

had a sticky morphology, indicating partial dissolution of the SEs by toluene, which accounted for the decreased Li^+ conductivities. In Figure 1f, representative processing solvents for sulfide SEs are summarized and evaluated in terms of safety, compatibility, and boiling point, in comparison with NMP (green line).

Polymeric binders

Polymeric binders maintain electrode integrity, making the electric networks continuous by binding the active materials, SEs, and conductive additives. They also alleviate the detrimental electrochemo-mechanical effects caused by the volumetric strain during repeated charge−discharge cycles [36−38]. However, because of the insulating property of polymeric binders, both Li^+ and e^- transports in ASLB electrodes are impeded, which is the main reason for the degraded electrochemical performance of sheet-type electrodes (Figure 2a) [18]. The differences in the discharge capacities of the electrodes with and without binders were 18−35 mA h g^{-1} for $LiNi_{0.6}Co_{0.2}Mn_{0.2}O_2$/Li−In half-cells at 0.1C and 30 °C. These results are consistent with those of following studies [39−42]. Zhang et al. investigated the effect of binder content on the electrochemical performance of $LiNi_{0.8}Co_{0.1}Mn_{0.1}O_2$ cathodes [40]. The composite cathodes using 1 wt.% ethyl cellulose showed better cell performance compared to those using 0.5 wt.% or > 1 wt.% ethyl cellulose. The presence of the optimum fraction of ethyl cellulose implies complementary cooperation between the intimate CAM/SE contacts and the Li^+ hindrance by the polymeric binders.

Three strategies have been proposed to address the problem stemming from the degraded Li^+ contact using polymeric binders. The first approach involves the elimination of the polymeric binders in the electrodes [22,43]. Yamamoto et al. reported the fabrication of binder-free sheet-type all-solid-state batteries (Figure 2b) [22]. The volatile poly(propylene carbonate) (PPC) used for electrode slurries could be depolymerized and quickly evaporated under vacuum at elevated temperature (225 °C). Thus, upon eliminating the binders, the CAM/SE interfacial resistance drastically decreased from 638 Ω to 14 Ω. This binder-free approach can also be applied to Si anodes [43]. The second strategy to mitigate the Li^+ contacts degraded by binders is to reduce the binder content by improving the adhesive properties of the binders. In other words, a highly adhesive binder can offer sufficient electrode integrity in small amounts. The absence of polar groups in polymeric binders, which are widely used for ASLBs, is disadvantageous for forming strong interactions with electrode active materials or current collectors [24]. To elaborately control the polarity of polymeric binders, Lee et al. developed to graft 3-mercaptocarboxylic acid into styrene-butadiene block-copolymers via a thiol−ene click reaction [44]. The polar −COOH moiety provides sufficient binding ability, which is superior to that of conventional PVdF. However, the new binders were insoluble in nonpolar solvents because of the large number of −COOH groups. Subsequent research suggested the use of polymers with a *tert*-butyl acrylate group to avoid polarity mismatch (Figure 2c) [45]. Initially, these binders were soluble in butyl butyrate with intermediate polarity because of the absence of a polar moiety. During the drying process, the nonpolar *tert*-butyl acrylate groups were thermally cleaved at 160 °C, and the polar −COOH moiety was deprotected. These deprotected polymeric binders increased the peeling strength of the electrodes by more than twofold (Figure 2d).

The final strategy for circumventing the degraded Li^+ contact by binders is to impart Li^+ conductivity to the binders [19,23,34,46]. Gel polymer electrolytes (GPEs) are attractive candidates. Oh et al. first demonstrated a slurry-fabricable Li^+-conductive polymeric binder using NBR and solvate ionic liquids (SILs) called "Li(G3)TFSI," where G3 is triethylene glycol dimethyl ether and LiTFSI is lithium bis(trifluoromethanesulfonyl) imide (Figure 2e) [19]. DBM successfully accommodated multiple components owing to its intermediate polarity, which allowed for marginal reactivity with sulfide SEs, dissolution of the binder NBR, and mixing with the SILs. The GPE-based binders effectively facilitated Li^+ contact and pathways throughout the electrodes. As a result, $LiNi_{0.70}Co_{0.15}Mn_{0.15}O_2$ electrodes using NBR-LiG3 achieved an ultrahigh mass loading of 45 mg cm^{-2}, showing a high areal capacity of 7.4 mA h cm^{-2}. However, electrodes using GPE-based binders delivered limited performance under thermally abusing conditions, which originated from the detrimental interaction between sulfide SEs and organic small molecules at elevated temperatures [23]. Moreover, SIL-based GPE binders were not compatible with graphite electrodes. These problems were resolved by developing thermally stable dry polymer electrolyte (DPE)-type binders [23,34]. The use of benzyl acetate as the processing solvent could aid in blending the binders (poly(1,4-butylene adipate) and NBR) and Li salts (LiTFSI) without damaging the sulfide SEs. The resulting DPE binders enabled highly improved electrochemical performance of both $LiNi_{0.70}Co_{0.15}Mn_{0.15}O_2$ cathodes and graphite anodes over a wide temperature range between −10 and 70 °C (Figure 2f) [23]. The use of cosolvents, in which two solvent molecules work synergistically for the dissolution of the binder NBR and the Li salt LiTFSI, also allowed the accommodation of DPE-type binders for ASLBs (Figure 2g) [34]. Specifically, the less-polar DBM and more polar HB acted as solvents for dissolving NBR and LiTFSI, respectively [34]. The Li^+-conductive NBR-LiTFSI derived using the DBM-HB cosolvents showed remarkably improved the electrochemical performance of $LiNi_{0.70}Co_{0.15}Mn_{0.15}O_2$ cathodes and graphite anodes at both 30 and 70 °C as

Figure 2

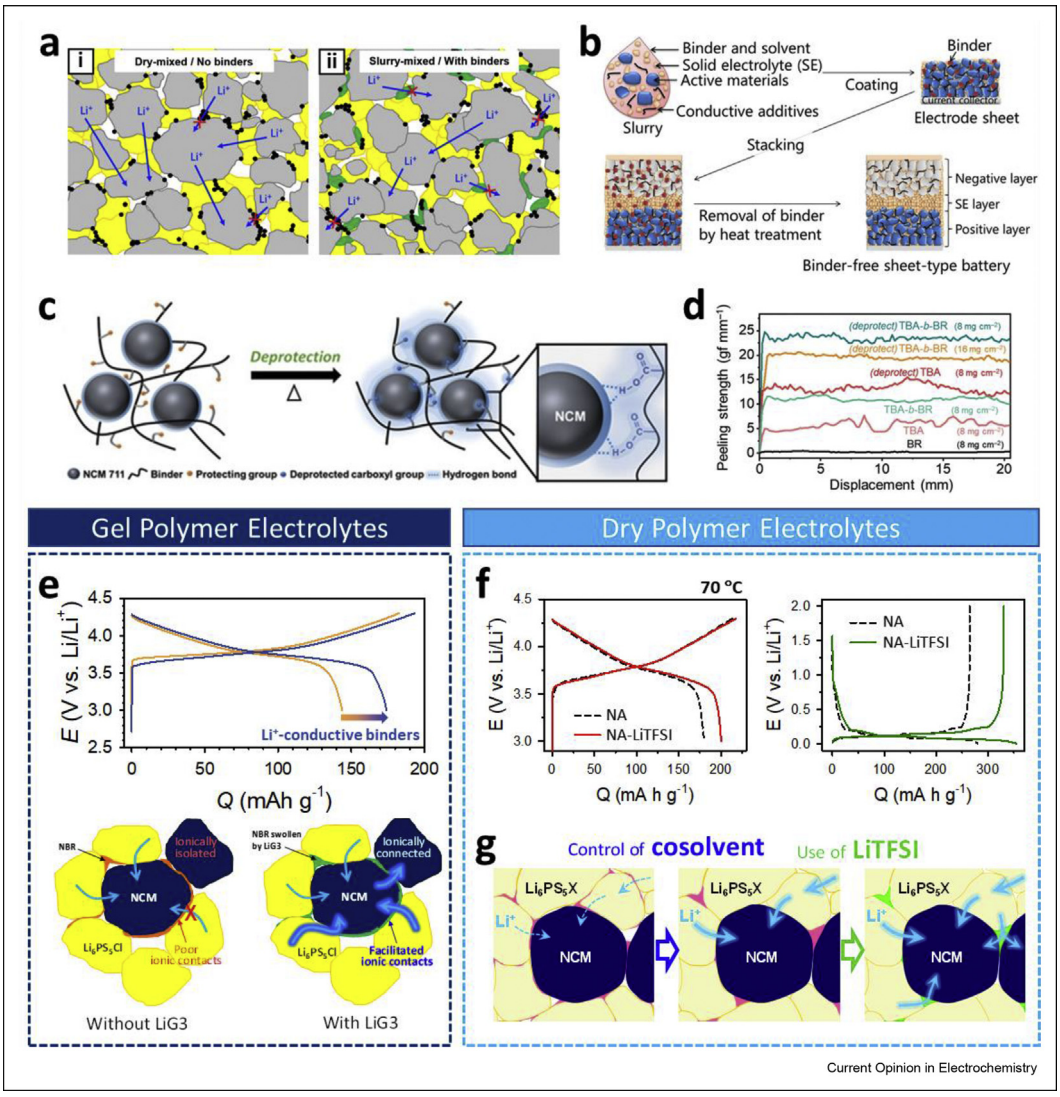

Developments of polymeric binders for sulfide SE-based ASLBs. (**a**) Schematic of the microstructure of ASLB electrodes prepared by dry-mixing without binders and by wet-slurry process using binders. Reproduced with permission from Ref. [18], Copyright 2018, Elsevier. (**b**) Schematic of the fabrication of binder-free sheet-type electrodes. Reproduced with permission from Ref. [22], Copyright 2018, Nature Publishing Group. (**c**) Schematic of the protection-deprotection chemistry for the adhesive interaction between binder and CAMs and (**d**) the corresponding 180° peeling test results. Reproduced with permission from Ref. [45], Copyright 2020, Wiley-VCH. (**e**) First-cycle charge–discharge voltage profiles of $LiNi_{0.70}Co_{0.15}Mn_{0.15}O_2$ (NCM) electrodes with and without LiG3, and schematic of the microstructure of NCM electrodes. Reproduced with permission from Ref. [19], Copyright 2019, Wiley-VCH. (**f**) First-cycle charge–discharge voltage profiles of NCM electrodes at 70 °C and graphite electrodes. Reproduced with permission from Ref. [23], Copyright 2021, Elsevier. (**g**) Schematic of the microstructure of NCM electrodes fabricated using DPE-type binder with cosolvents DBM + HB. Reproduced with permission from Ref. [34], Copyright 2021, Wiley-VCH.

compared to that when using the conventional Li^+-insulating binder NBR.

The interaction between the sulfide SEs and polymeric binders is also a design factor to be considered for sheet-type ASLB electrodes. X-ray photoelectron spectroscopy (XPS) measurements of the NBR/($75Li_2S$–$25P_2S_5$) composite materials revealed ion–dipole interactions that resulted in good dispersion of the NBR binder and played a key role in facilitating Li^+ transport more efficiently as compared to BR/($75Li_2S$–$25P_2S_5$) [21]. However, the weakened bond energy of Li with polymers degrades the chemical stability of sulfide SEs. Teo et al. reported that hydrogenated NBR (h-NBR) embedded in $LiNi_{0.6}Co_{0.2}Mn_{0.2}O_2$ electrodes produced the highest amount of SO_2 among polyisobutene, SBR, and h-NBR [42]. In addition, Riphaus et al. reported the chemical degradation of $Li_{10}SnP_2S_{12}$ by poly(ethylene oxide)

(PEO)-LiTFSI [47]. The EIS results revealed that the resistance of interface between LSPS and $PEO_{15}LiTFSI$ gradually increased over time at 40 °C.

Electrochemical stability of polymeric binders also affects the electrochemical performance of ASLBs. At high voltages, $LiNi_{0.6}Co_{0.2}Mn_{0.2}O_2$ releases reactive O_2 from the lattice, and CO_2 is also evolved by chemical oxidation of binders [42,48]. Interestingly, cathodes using SBR-based binders exhibited 2–3 times more CO_2 evolution than those using polyisobutene-based binders, which emphasizes the importance of selecting binders in terms of the electrochemical stability.

Alternative wet-fabrication for ASLBs

Jung group developed several solution-processable sulfide SE chemistries, such as (LiI)–Li_4SnS_4 using methanol (MeOH) or water [49], $Li_{6-x}PS_{5-x}[Cl,Br]_x$ or $Li_{6+x}P_{1-x}M_xS_5I$ (M = Ge, Sn) using ethanol (EtOH) [50–52], and Na_3SbS_4 using water or MeOH [53]. In the solution process, sulfide SEs are fully dissolved to form homogeneous solutions, and the original SEs are precipitated under vacuum and subsequent heat treatment. The solution process offers alternative fabrication protocols for sheet-type electrodes for ASLBs, with the additional benefit of intimate ionic contact [49,50,54]. Liquified Li_6PS_5Cl using EtOH infiltrated porous composite electrodes that were prepared using PVDF and NMP for conventional LIBs (Figure 3a). ASLB electrodes could be prepared by subsequent drying, heat treatment, and cold pressing. Despite the insufficient Li^+ conductivities of the solution-processed SEs (~0.1 mS cm^{-1}), the resulting $LiCoO_2$ and graphite electrodes showed high reversible capacities of 141 and 364 mA h g^{-1} at 0.1C and 30 °C, respectively, which were comparable to those of liquid electrolyte cells (Figure 3b). In addition, the low weight fraction of inactive components, including SEs (~12 wt.% for $LiCoO_2$ and ~21 wt.% for Gr), polymeric binders, and carbon additives, demonstrates the effectiveness of forming ionic conduction pathways and the practical importance of the infiltration protocol. This infiltration protocol for ASLBs was also adaptable to thin SE membranes and Si anodes [50,52,55]. Furthermore, another class of SE, closo-borate $Na_4(B_{12}H_{12})(B_{10}H_{10})$, with a high ionic conductivity of 1 mS cm^{-1} at 25 °C, was also demonstrated to allow the infiltration-based fabrication of all-solid-state Na-ion battery electrodes [56].

Alternatively, sheet-type electrodes can be prepared using SE precursors rather than the prepared SEs. Oh et al. demonstrated a single-step wet-chemical fabrication of sheet-type electrodes using Li_2S and P_2S_5 as SE precursors, and tetrahydrofuran as both the processing solvent and reaction media [54]. Electrode active materials, binders, and conducting additives were also added. The wet-synthesis of Li_3PS_4 proceeded *in situ* during the electrode fabrication process, that is, slurry mixing, casting, and drying at elevated temperatures (Figure 3c). At 30 °C, the $LiNi_{0.6}Co_{0.2}Mn_{0.2}O_2$ and graphite electrodes exhibited reasonably good capacities

Figure 3

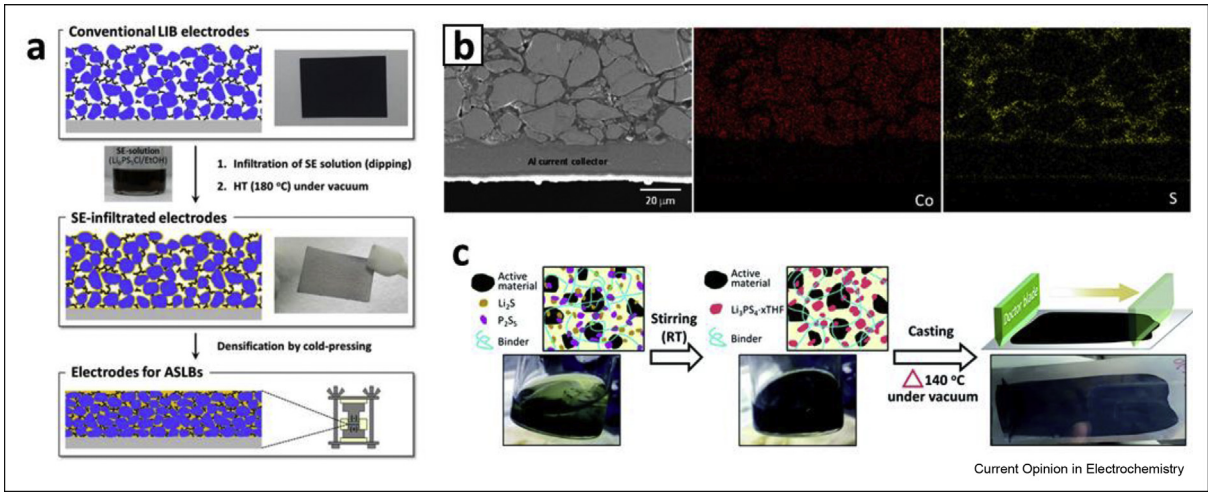

Alternative wet-fabrication strategies for sulfide SE-based ASLBs. (**a**) Schematic illustration of the infiltration of conventional LIB composite electrodes with solution-processable SEs and (**b**) corresponding cross-sectional SEM image of the electrodes with the EDX elemental maps. Reproduced with permission from Ref. [50], Copyright 2017, American Chemical Society. (**c**) Schematic of the single-step wet-fabrication of sheet-type composite electrodes. Reproduced with permission from Ref. [54], Copyright 2017, Royal Society of Chemistry.

of 140 mA h g^{-1} (0.1C) and 320 mA h g^{-1} (0.2C), respectively.

Kato et al. designed Li^+-conductive sulfide polymer electrolytes with a Li^+ conductivity of 3.0×10^{-5} S cm^{-1}, targeting binders for sheet-type ASLB electrodes. Li_3PS_4 was polymerized via ball milling using I_2. The reaction of the two PS_4^{3-} anions with I_2 afforded a dimer comprising two PS_4 tetrahedra bridged with a disulfide bond and continuously constructed the polysulfide structure $(\text{-P-S-S-})_n$. Using Li^+-conductive sulfide polymer electrolytes, all-inorganic solid electrolyte membranes and electrodes were fabricated. The resulting $LiNi_{1/3}Co_{1/3}Mn_{1/3}O_2$ electrodes showed a capacity retention of 93.8% at the 200th cycle compared to the capacity at the 5th cycle [57].

Dry-film fabrication for ASLBs

The wet-slurry fabrication of ASLBs is attractive because it can utilize mature manufacturing LIB infrastructures. However, several drawbacks are associated with the use of solvents. The degradation of sulfide SEs by solvents is inevitable, although marginal. From a practical point of view, the solvents themselves and their drying processes are costly and are estimated to be approximately 8–9% of the total pack cost for NMP [58,59]. In addition, the fabrication of thick electrodes using the wet-slurry method requires large amounts of polymeric binders and a low drying rate [32,60]. Recently, an alternative dry-film fabrication protocol has been emerging to address these disadvantages of the wet-slurry methods. The elimination of any solvent makes dry-film fabrication highly profitable in terms of both electrochemical performance and cost. Moreover, even with small amounts of polymers, thick electrodes can be fabricated using dry-film fabrication. In this section, recent research on dry-film fabrication of ASLBs is briefly summarized and discussed.

Hippauf et al. first reported the solvent-free dry-film fabrication of sheet-type ASLB electrodes [61]. Free-standing sheet-type electrodes can be fabricated by

Figure 4

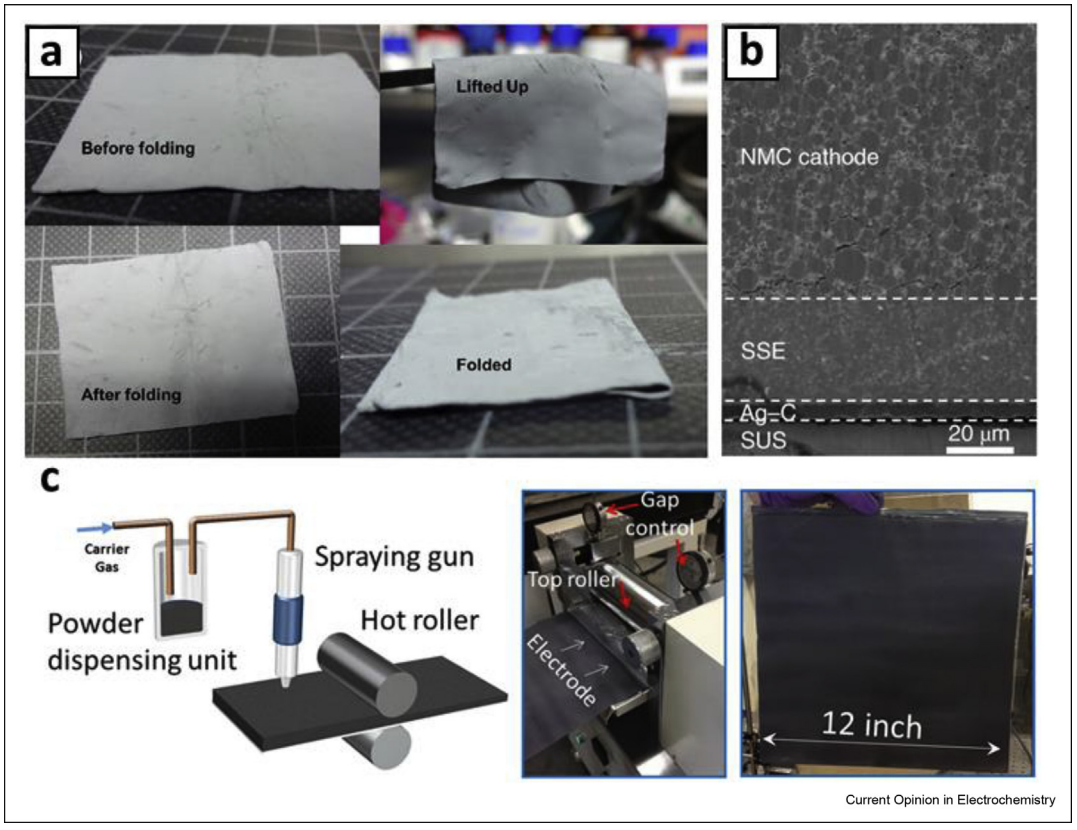

Dry-film fabrication of sulfide SE-based ASLBs and LIBs. (**a**) Photographs of a 4.0 × 3.5 cm^2 $LiNi_{0.9}Co_{0.05}Mn_{0.05}O_2$ electrode with 0.3 wt.% PTFE. Reproduced with permission from Ref. [61], Copyright 2019, Elsevier. (**b**) Cross-sectional SEM image of the ASLB structure comprising NCM electrode with 1 wt.% PTFE, sulfide SE layer, Ag–C layer, and SUS current collector. Reproduced with permission from Ref. [5], Copyright 2020, Nature Publishing Group. (**c**) Schematic and photographs of the manufacturing system of electrodes created by dry particle painting processes. Reproduced with permission from Ref. [66], Copyright 2016, Nature Publishing Group.

mixing CAMs, SEs, and carbon additives using polytetrafluoroethylene (PTFE) in a heated mortar. Dry-film fabrication is enabled by the characteristic transformation of PTFE beads to fibrils, that is, from a triclinic to a hexagonal crystalline lattice upon heating above 19 °C. The hexagonal crystalline lattice is more deformable than the triclinic lattice. Thus, PTFE can be easily fibrillated by external shearing forces, particularly at high temperatures [62]. The fibril and spider-web morphology of PTFE effectively holds the CAM and SE particles together. Therefore, the PTFE amount could reach a minimum of 0.1 wt.%. Figure 4a shows the free-standing electrodes fabricated by the dry method using PTFE. The absence of degradation caused by solvents and minimal Li^+ hindrance by binders led to a high areal capacity of 6.5 mA h cm^{-2}. In addition, a pouch-type full cell with a capacity of 21 mA h was successfully demonstrated.

The potential of dry-film fabrication has opened an avenue for practical high-energy ASLB electrodes [5,6,63,64]. In 2020, Lee et al. reported Li-metal-free ASLBs enabled by Ag–C composite anodes [5]. The Ag–C layer could effectively reduce the nucleation energy for the formation and uniform deposition of Li metal on current collectors. A prototype pouch cell showed high energy density of >900 Wh L^{-1} and excellent capacity retention of 89% after 1000 cycles. Importantly, a high-areal-capacity cathode (>6.8 mA h cm^{-2}) was prepared by dry-film fabrication. The thickness of the prepared electrodes was approximately 100 μm. Tan et al. showed that Si anodes with a 99.9 wt.% micrometer-sized could operate $LiNi_{0.8}Co_{0.1}Mn_{0.1}O_2$/Si all-solid-state full cells with a stable capacity retention of 80% after 500 cycles [6]. Notably, the full cells employed a high-areal-capacity cathode (12 mA h cm^{-2}) prepared by dry-film fabrication. Very recently, Hong et al. designed PTFE-based Li^+-conducting ionomer for dry-processed composite cathodes [65]. Lithium salt perfluoro(3-oxa-4-pentenesulfonic acid) facilitates Li^+ transports and ensures good interfacial contact between the $Li_{0.7}Co_{0.1}Mn_{0.2}O_2$ and Li_6PS_5Cl, consistent with previous results using Li^+-conductive binders of ASLBs [19,23,34,46].

Despite their potential to enable the high energy density of ASLBs, the dry-fabrication technology is in its infancy. Specifically, electrodes must be fabricated with homogeneous and uniform thickness using scalable protocols. In this regard, the use of a hot roller is advantageous [66,67]. Moreover, by using a hot roller, thermal activation of the binding material PTFE is quickly achieved. Incorporating a small amount of SE-compatible solvents such as dehydrated xylene may also be an alternative strategy [5]. Although manual mixing in a heated mortar has been used for lab-scale dry-film fabrication, alternative mixing strategies, such as those using a homogenizer, vortex mixer, and ball-milling, should be investigated as already demonstrated as a proof-of-concept for conventional LIB

Figure 5

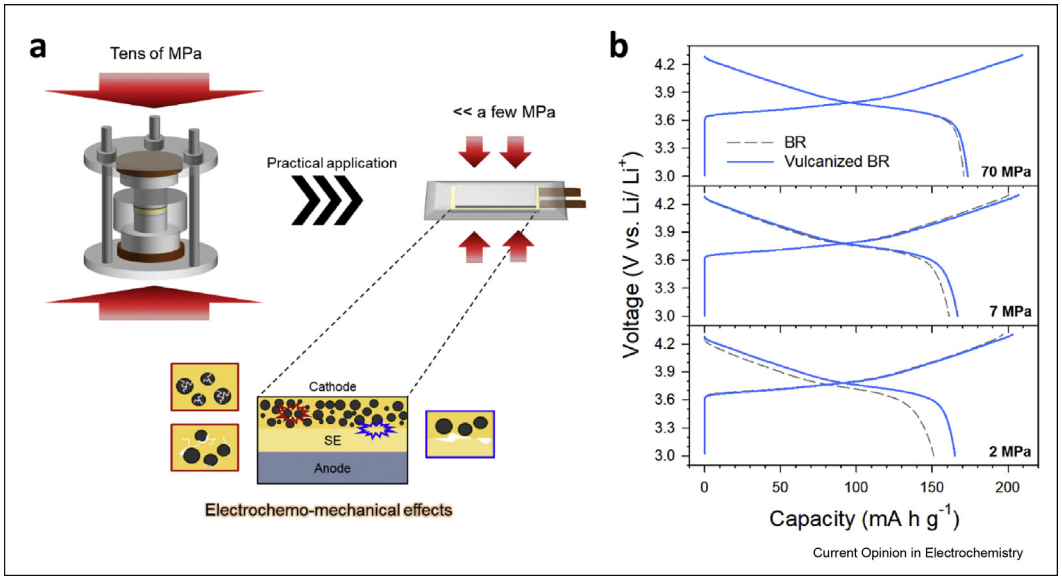

Effects of polymeric binders for ASLB cells operating at low external pressures. (**a**) Schematic of ASLB cells operating at high and low pressures, and their relevant electrochemo-mechanical effects. (**b**) First-cycle charge–discharge voltage profiles of $LiNi_{0.70}Co_{0.15}Mn_{0.15}O_2$/Li–In cells at 0.1C and 30 °C using pristine or vulcanized BR under various external operating pressures (70, 7, 2 MPa). Reproduced with permission from Ref. [72], Copyright 2022, Elsevier.

systems [66,68,69]. However, to induce the characteristic transformation of PTFE beads into fibrils, strong shearing forces are required, which calls for customized processes. Zhang et al. reported a ball-milling strategy to mix $Li_{5.4}PS_{4.4}Cl_{1.6}$ and PTFE by shearing PTFE fibers [70]. The prepared thin SE membranes with a thickness of ~30 μm exhibited a high room temperature conductivity of 8.4 mS cm^{-1} with a flexible feature. If scalable mixing can be achieved, continuous dry-film fabrication strategies should be followed (Figure 4c). For instance, hot-pressing, extrusion, and electrostatic spray deposition are worth noting for ASLBs. Extrusion is advantageous because of its high shear rates and scalability, but it requires the use of solvents or elevated temperatures. Electrostatic spray deposition is a solvent-free and versatile approach, but in this case, it is difficult to control the electrode thickness [66,67,71].

Concluding remarks

Research on novel sulfide Li^+ superionic conductors with high Li^+ conductivities has triggered the development of ASLBs with improved safety and energy densities. However, the success of practical ASLBs is not achieved solely by the high Li^+ conductivity of the SEs. A basic understanding of interfacial (electro)chemical reactions, chemical stability, and solid–solid contact under electrochemo-mechanically driven stresses, as well as comprehensive practical considerations on scalable fabrication strategies for electrodes and SE membranes should follow. The wet-slurry method is highly competitive in terms of fabrication at scale and can adopt the well-developed infrastructure of conventional LIBs with minimal alteration. However, the degradation of sulfide SEs by the solvents and Li^+-insulating properties of polymeric binders inevitably degrades the electrochemical performance of ASLBs. Thus, careful selection and blending of solvents and functional polymeric binders are necessary to tailor sulfide SEs. Slurry-processing solvents should possess a low polarity that is sufficiently benign to vulnerable sulfide SEs, adequate vapor pressure and boiling points, nontoxicity, and dissolving ability of polymeric binders (and Li salts for application to Li^+-conductive binders). Polymeric binders should offer sufficiently high adhesion and resilient physical properties to alleviate electrochemo-mechanical stresses. Recently, Kwon et al. developed 3D networking binders prepared *in situ* during the wet-slurry process via vulcanization (Figure 5) [72]. It was first demonstrated that electrochemical performance under a practically acceptable low external pressure of 2 MPa for $LiNi_{0.70}Co_{0.15}Mn_{0.15}O_2$ electrodes was significantly enhanced by using vulcanized BR. This is in sharp contrast to the marginal differences in performance at an unrealistic operating pressure of 70 MPa, enlightening research direction for the development of scalable functional binders for sulfide-based ASLBs. In addition, the mechanical property of SEs should be considered to alleviate electrochemo-mechanical stresses in sheet-type electrodes [48]. The dry-film fabrication strategy is highly promising in terms of the electrochemical performance of the resulting ASLB cells. This is because of the absence of reactive organic solvents and the excellent formability that can minimize the binder amount to as low as 0.1 wt.%. In particular, the ability to fabricate ultrathick electrodes without significant delamination is a crucial advantage of dry-film fabrication for realizing ASLBs with high energy density. However, for scalable fabrication, intensive developments, such as mixing, deposition, and calendaring, are required, which may also address the inhomogeneity problems in electrode thickness and distribution of components. Specifically, while calendaring by roll-press is highly attractive for the large-scale fabrication, non-uniform powder compaction needs to be addressed [73]. Moreover, mechanical properties and degradation of electrodes, altered by fabricating pressures, are an intriguing issue for future research [31,37,74–76].

Declaration of competing interest

The authors declare that they have no known competing financial interests or personal relationships that could have appeared to influence the work reported in this paper.

Acknowledgements

This work was supported by the Technology Development Program to Solve Climate Changes and by the Basic Science Research Program through the National Research Foundation of Korea funded by the Ministry of Science, ICT & Future Planning (NRF-2018R1A2B6004996 and 2017M1A2A2044501), and by the Materials and Components Technology Development Program of MOTIE/KEIT (grant no. 20007045 and 20012216). The work was also funded by the Yonsei University Research Fund of 2021 (2021-22-0326).

References

Papers of particular interest, published within the period of review, have been highlighted as:

* of special interest
** of outstanding interest

1. Choi JW, Aurbach D: **Promise and reality of post-lithium-ion batteries with high energy densities**. *Nat Rev Mater* 2016, **1**: 16013.

2. Zeng X, Li M, Abd El-Hady D, Alshitari W, Al-Bogami AS, Lu J, Amine K: **Commercialization of lithium battery technologies for electric vehicles**. *Adv Energy Mater* 2019, **9**:1900161.

3. Li M, Wang C, Chen Z, Xu K, Lu J: **New concepts in electrolytes**. *Chem Rev* 2020, **120**:6783–6819.

4. Park KH, Bai Q, Kim DH, Oh DY, Zhu Y, Mo Y, Jung YS: **Design strategies, practical considerations, and new solution processes of sulfide solid electrolytes for all-solid-state batteries**. *Adv Energy Mater* 2018, **8**:1800035.

5. Lee Y-G, Fujiki S, Jung C, Suzuki N, Yashiro N, Omoda R, Ko D-S, Shiratsuchi T, Sugimoto T, Ryu S, Ku JH, Watanabe T, Park Y, Aihara Y, Im D, Han IT: **High-energy long-cycling all-solid-state lithium metal batteries enabled by silver–carbon composite anodes**. *Nat Energy* 2020, **5**:299–308.

6. Tan DHS, Chen Y-T, Yang H, Bao W, Sreenarayanan B, Doux J-M, Li W, Lu B, Ham S-Y, Sayahpour B, Scharf J, Wu EA, Deysher G, Han HE, Hah HJ, Jeong H, Lee JB, Chen Z, Meng YS:

Carbon-free high-loading silicon anodes enabled by sulfide solid electrolytes. *Science* 2021, **373**:1494–1499.

7. Janek J, Zeier WG: **A solid future for battery development**. *Nat Energy* 2016, **1**:16141.

8. Kato Y, Hori S, Saito T, Suzuki K, Hirayama M, Mitsui A, Yonemura M, Iba H, Kanno R: **High-power all-solid-state batteries using sulfide superionic conductors**. *Nat Energy* 2016, **1**:16030.

9. Zhao Q, Stalin S, Zhao C-Z, Archer LA: **Designing solid-state electrolytes for safe, energy-dense batteries**. *Nat Rev Mater* 2020, **5**:229–252.

10. Bocharova V, Sokolov AP: **Perspectives for polymer electrolytes: a view from fundamentals of ionic conductivity**. *Macromolecules* 2020, **53**:4141–4157.

11. Huo H, Huang K, Luo W, Meng J, Zhou L, Deng Z, Wen J, Dai Y, Huang Z, Shen Y, Guo X, Ji X, Huang Y: **Evaluating interfacial stability in solid-state pouch cells via ultrasonic imaging**. *ACS Energy Lett* 2022, **7**:650–658.

12. Adeli P, Bazak JD, Park KH, Kochetkov I, Huq A, Goward GR, Nazar LF: **Boosting solid-state diffusivity and conductivity in lithium superionic argyrodites by halide substitution**. *Angew Chem Int Ed* 2019, **58**:8681–8686.

13. Stramare S, Thangadurai V, Weppner W: **Lithium lanthanum titanates: a review**. *Chem Mater* 2003, **15**:3974–3990.

14. Asano T, Sakai A, Ouchi S, Sakaida M, Miyazaki A, Hasegawa S: **Solid halide electrolytes with high lithium-ion conductivity for application in 4 V class bulk-type All-solid-state batteries**. *Adv Mater* 2018, **30**:1803075.

15. Kim S, Oguchi H, Toyama N, Sato T, Takagi S, Otomo T, Arunkumar D, Kuwata N, Kawamura J, Orimo S-i: **A complex hydride lithium superionic conductor for high-energy-density all-solid-state lithium metal batteries**. *Nat Commun* 2019, **10**:1081.

16. Sakuda A, Hayashi A, Tatsumisago M: **Sulfide solid electrolyte with favorable mechanical property for all-solid-state lithium battery**. *Sci Rep* 2013, **3**:2261.

17. Banerjee A, Wang X, Fang C, Wu EA, Meng YS: **Interfaces and interphases in all-solid-state batteries with inorganic solid electrolytes**. *Chem Rev* 2020, **120**:6878–6933.

18. ** Nam YJ, Oh DY, Jung SH, Jung YS: **Toward practical all-solid-state lithium-ion batteries with high energy density and safety: comparative study for electrodes fabricated by dry- and slurry-mixing processes**. *J Power Sources* 2018, **375**:93–101.
This work reported a comparative study for electrodes fabricated by dry- and slurry-mixing processes, which revealed the Li+-blocking behavior of polymeric binders in electrodes.

19. * Oh DY, Nam YJ, Park KH, Jung SH, Kim KT, Ha AR, Jung YS: **Slurry-fabricable Li^+-Conductive polymeric binders for practical all-solid-state lithium-ion batteries enabled by solvate ionic liquids**. *Adv Energy Mater* 2019, **9**:1802927.
This work reported Li^+-conductive gel polymer electrolytes as polymeric binders for sheet-type ASLB electrodes using sulfide SEs.

20. Muramatsu H, Hayashi A, Ohtomo T, Hama S, Tatsumisago M: **Structural change of Li_2S–P_2S_5 sulfide solid electrolytes in the atmosphere**. *Solid State Ionics* 2011, **182**:116–119.

21. ** Lee K, Kim S, Park J, Park SH, Coskun A, Jung DS, Cho W, Choi JW: **Selection of binder and solvent for solution-processed all-solid-state battery**. *J Electrochem Soc* 2017, **164**:A2075–A2081.
This work reported the selection strategies of binder and solvent for sulfide solid electrolyte-based ASLBs.

22. * Yamamoto M, Terauchi Y, Sakuda A, Takahashi M: **Binder-free sheet-type all-solid-state batteries with enhanced rate capabilities and high energy densities**. *Sci Rep* 2018, **8**:1212.
This work reported binder-free sheet-type ASLB electrodes using combustible poly(propylene carbonate).

23. Oh DY, Kim KT, Jung SH, Kim DH, Jun S, Jeoung S, Moon HR, Jung YS: **Tactical hybrids of Li^+-conductive dry polymer electrolytes with sulfide solid electrolytes: toward practical all-solid-state batteries with wider temperature operability**. *Mater Today* 2021, https://doi.org/10.1016/j.mattod.2021.01.006.

24. Chen H, Ling M, Hencz L, Ling HY, Li G, Lin Z, Liu G, Zhang S: **Exploring chemical, mechanical, and electrical functionalities of binders for advanced energy-storage devices**. *Chem Rev* 2018, **118**:8936–8982.

25. * Inada T, Kobayashi T, Sonoyama N, Yamada A, Kondo S, Nagao M, Kanno R: **All solid-state sheet battery using lithium inorganic solid electrolyte, thio-LISICON**. *J Power Sources* 2009, **194**:1085–1088.
This work firstly reported the prototype configruation and fabrication process for pouch-type ASLB cells.

26. Ito S, Fujiki S, Yamada T, Aihara Y, Park Y, Kim TY, Baek S-W, Lee J-M, Doo S, Machida N: **A rocking chair type all-solid-state lithium ion battery adopting Li_2O–ZrO_2 coated $LiNi_{0.8}Co_{0.15}Al_{0.05}O_2$ and a sulfide based electrolyte**. *J Power Sources* 2014, **248**:943–950.

27. Sakuda A, Kuratani K, Yamamoto M, Takahashi M, Takeuchi T, Kobayashi H: **All-solid-state battery electrode sheets prepared by a slurry coating process**. *J Electrochem Soc* 2017, **164**:A2474–A2478.

28. Riphaus N, Strobl P, Stiaszny B, Zinkevich T, Yavuz M, Schnell J, Indris S, Gasteiger HA, Sedlmaier SJ: **Slurry-based processing of solid electrolytes: a comparative binder study**. *J Electrochem Soc* 2018, **165**:A3993–A3999.

29. Ates T, Keller M, Kulisch J, Adermann T, Passerini S: **Development of an all-solid-state lithium battery by slurry-coating procedures using a sulfidic electrolyte**. *Energy Storage Mater* 2019, **17**:204–210.

30. Hatz A-K, Calaminus R, Feijoo J, Treber F, Blahusch J, Lenz T, Reichel M, Karaghiosoff K, Vargas-Barbosa NM, Lotsch BV: **Chemical stability and ionic conductivity of LGPS-type solid electrolyte tetra-Li_7SiPS_8 after solvent treatment**. *ACS Appl Energy Mater* 2021, **4**:9932–9943.

31. Yamamoto M, Takahashi M, Terauchi Y, Kobayashi Y, Ikeda S, Sakuda A: **Fabrication of composite positive electrode sheet with high active material content and effect of fabrication pressure for all-solid-state battery**. *J Ceram Soc Jpn* 2017, **125**:391–395.

32. Jaiser S, Müller M, Baunach M, Bauer W, Scharfer P, Schabel W: **Investigation of film solidification and binder migration during drying of Li-Ion battery anodes**. *J Power Sources* 2016, **318**:210–219.

33. Chen K, Shinjo S, Sakuda A, Yamamoto K, Uchiyama T, Kuratani K, Takeuchi T, Orikasa Y, Hayashi A, Tatsumisago M, Kimura Y, Nakamura T, Amezawa K, Uchimoto Y: **Morphological effect on reaction distribution influenced by binder materials in composite electrodes for sheet-type All-solid-state lithium-ion batteries with the sulfide-based solid electrolyte**. *J Phys Chem C* 2019, **123**:3292–3298.

34. * Kim KT, Oh DY, Jun S, Song YB, Kwon TY, Han Y, Jung YS: **Tailoring slurries using cosolvents and Li salt targeting practical all-solid-state batteries employing sulfide solid electrolytes**. *Adv Energy Mater* 2021, **11**:2003766.
This work reported cosolvent systems to accommodate Li^+-conductive dry polymer electrolytes as polymeric binders and control their distribution for sheet-type ASLB electrodes.

35. Ruhl J, Riegger LM, Ghidiu M, Zeier WG: **Impact of solvent treatment of the superionic argyrodite Li_6PS_5Cl on solid-state battery performance**. *Adv Sustain Syst* 2021, **2**:2000077.

36. Choi S, Kwon T-w, Coskun A, Choi Jang W: **Highly elastic binders integrating polyrotaxanes for silicon microparticle anodes in lithium ion batteries**. *Science* 2017, **357**:279–283.

37. Hu L, Zhang X, Zhao P, Fan H, Zhang Z, Deng J, Ungar G, Song J: **Gradient H-bonding binder enables stable high-areal-capacity Si-based anodes in pouch cells**. *Adv Mater* 2021, **33**:2104416.

38. Bae Song Y, Kwak H, Cho W, Kim KS, Seok Jung Y, Park K-H: **Electrochemo-mechanical effects as a critical design factor for all-solid-state batteries**. *Curr Opin Solid State Mater Sci* 2022, **26**:100977.

39. Rosero-Navarro NC, Kinoshita T, Miura A, Higuchi M, Tadanaga K: **Effect of the binder content on the electrochemical performance of composite cathode using Li_6PS_5Cl precursor solution in an all-solid-state lithium battery**. *Ionics* 2017, **23**:1619–1624.

40. Zhang J, Zhong H, Zheng C, Xia Y, Liang C, Huang H, Gan Y, Tao X, Zhang W: **All-solid-state batteries with slurry coated $LiNi_{0.8}Co_{0.1}Mn_{0.1}O_2$ composite cathode and Li_6PS_5Cl electrolyte: effect of binder content**. *J Power Sources* 2018, **391**: 73–79.

41. Bielefeld A, Weber DA, Janek J: **Modeling effective ionic conductivity and binder influence in composite cathodes for all-solid-state batteries**. *ACS Appl Mater Interfaces* 2020, **12**: 12821–12833.

42. Teo JH, Strauss F, Tripković Đ, Schweidler S, Ma Y, Bianchini M, Janek J, Brezesinski T: **Design-of-experiments-guided optimization of slurry-cast cathodes for solid-state batteries**. *Cell Rep Phys Sci* 2021:100465.

43. Yamamoto M, Terauchi Y, Sakuda A, Takahashi M: **Slurry mixing for fabricating silicon-composite electrodes in all-solid-state batteries with high areal capacity and cycling stability**. *J Power Sources* 2018, **402**:506–512.

44. * Lee K, Lee J, Choi S, Char K, Choi JW: **Thiol–ene click reaction for fine polarity tuning of polymeric binders in solution-processed all-solid-state batteries**. *ACS Energy Lett* 2019, **4**: 94–101.

This work reported polarity-tunable polymeric binders, which directly affect adheison proeprties, via thiol–ene reaction.

45. Lee J, Lee K, Lee T, Kim H, Kim K, Cho W, Coskun A, Char K, Choi JW: **In situ deprotection of polymeric binders for solution-processible sulfide-based all-solid-state batteries**. *Adv Mater* 2020, **32**:2001702.

46. Cho W, Park J, Kim K, Yu J-S, Jeong G: **Sulfide-compatible conductive and adhesive glue-like interphase engineering for sheet-type All-solid-state battery**. *Small* 2021, **17**:1902138.

47. Riphaus N, Stiaszny B, Beyer H, Indris S, Gasteiger HA, Sedlmaier SJ: **Editors' choice—understanding chemical stability issues between different solid electrolytes in all-solid-state batteries**. *J Electrochem Soc* 2019, **166**:A975–A983.

48. Teo JH, Strauss F, Walther F, Ma Y, Payandeh S, Scherer T, Bianchini M, Janek J, Brezesinski T: **The interplay between (electro)chemical and (chemo)mechanical effects in the cycling performance of thiophosphate-based solid-state batteries**. *Mater Future* 2022, **1**, 015102.

49. Park KH, Oh DY, Choi YE, Nam YJ, Han L, Kim J-Y, Xin H, Lin F, Oh SM, Jung YS: **Solution-processable glass LiI-Li_4SnS_4 superionic conductors for all-solid-state Li-ion batteries**. *Adv Mater* 2016, **28**:1874–1883.

50. ** Kim DH, Oh DY, Park KH, Choi YE, Nam YJ, Lee HA, Lee S-M, Jung YS: **Infiltration of solution-processable solid electrolytes into conventional Li-Ion-Battery electrodes for all-solid-state Li-ion batteries**. *Nano Lett* 2017, **17**:3013–3020.

This work reported an infiltration fabrication protocol using solution-processable sulfide solid electrolytes for ASLB electrodes.

51. Song YB, Kim DH, Kwak H, Han D, Kang S, Lee JH, Bak S-M, Nam K-W, Lee H-W, Jung YS: **Tailoring solution-processable Li argyrodites Li6+xP1–xMxS5I (M = Ge, Sn) and their microstructural evolution revealed by cryo-TEM for all-solid-state batteries**. *Nano Lett* 2020, **20**:4337–4345.

52. Kim DH, Lee Y-H, Song YB, Kwak H, Lee S-Y, Jung YS: **Thin and flexible solid electrolyte membranes with ultrahigh thermal stability derived from solution-processable Li argyrodites for all-solid-state Li-ion batteries**. *ACS Energy Lett* 2020, **5**:718–727.

53. Banerjee A, Park KH, Heo JW, Nam YJ, Moon CK, Oh SM, Hong S-T, Jung YS: **Na_3SbS_4: a solution processable sodium superionic conductor for all-solid-state sodium-ion batteries**. *Angew Chem Int Ed* 2016, **55**:9634–9638.

54. Oh DY, Kim DH, Jung SH, Han J-G, Choi N-S, Jung YS: **Single-step wet-chemical fabrication of sheet-type electrodes from solid-electrolyte precursors for all-solid-state lithium-ion batteries**. *J Mater Chem A* 2017, **5**:20771–20779.

55. Kim DH, Lee HA, Song YB, Park JW, Lee S-M, Jung YS: **Sheet-type Li_6PS_5Cl-infiltrated Si anodes fabricated by solution process for all-solid-state lithium-ion batteries**. *J Power Sources* 2019, **426**:143–150.

56. Duchêne L, Kim DH, Song YB, Jun S, Moury R, Remhof A, Hagemann H, Jung YS, Battaglia C: **Crystallization of closo-borate electrolytes from solution enabling infiltration into slurry-casted porous electrodes for all-solid-state batteries**. *Energy Storage Mater* 2020, **26**:543–549.

57. Kato A, Yamamoto M, Utsuno F, Higuchi H, Takahashi M: **Lithium-ion-conductive sulfide polymer electrolyte with disulfide bond-linked PS_4 tetrahedra for all-solid-state batteries**. *Commun Mater* 2021, **2**:112.

58. Zhang YS, Courtier NE, Zhang Z, Liu K, Bailey JJ, Boyce AM, Richardson G, Shearing PR, Kendrick E, Brett DJL: **A review of lithium-ion battery electrode drying: mechanisms and metrology**. *Adv Energy Mater* 2022, **12**:2102233.

59. Wood DL, Quass JD, Li J, Ahmed S, Ventola D, Daniel C: **Technical and economic analysis of solvent-based lithium-ion electrode drying with water and NMP**. *Dry Technol* 2018, **36**:234–244.

60. Westphal BG, Kwade A: **Critical electrode properties and drying conditions causing component segregation in graphitic anodes for lithium-ion batteries**. *J Energy Storage* 2018, **18**:509–517.

61. ** Hippauf F, Schumm B, Doerfler S, Althues H, Fujiki S, Shiratsuchi T, Tsujimura T, Aihara Y, Kaskel S: **Overcoming binder limitations of sheet-type solid-state cathodes using a solvent-free dry-film approach**. *Energy Storage Mater* 2019, **21**:390–398.

This work reported solvent-free dry-film fabrication strategies for ASLB electrodes.

62. Brown EN, Dattelbaum DM: **The role of crystalline phase on fracture and microstructure evolution of polytetrafluoroethylene (PTFE)**. *Polymer* 2005, **46**:3056–3068.

63. Cangaz S, Hippauf F, Reuter FS, Doerfler S, Abendroth T, Althues H, Kaskel S: **Enabling high-energy solid-state batteries with stable Anode interphase by the use of columnar silicon anodes**. *Adv Energy Mater* 2020, **10**:2001320.

64. Wang C, Yu R, Duan H, Lu Q, Li Q, Adair KR, Bao D, Liu Y, Yang R, Wang J, Zhao S, Huang H, Sun X: **Solvent-free approach for interweaving freestanding and ultrathin inorganic solid electrolyte membranes**. *ACS Energy Lett* 2022, **7**: 410–416.

65. Hong S-B, Lee Y-J, Kim U-H, Bak C, Lee YM, Cho W, Hah HJ, Sun Y-K, Kim D-W: **All-solid-state lithium batteries: Li^+-Conducting ionomer binder for dry-processed composite cathodes**. *ACS Energy Lett* 2022:1092–1100.

66. Ludwig B, Zheng Z, Shou W, Wang Y, Pan H: **Solvent-free manufacturing of electrodes for lithium-ion batteries**. *Sci Rep* 2016, **6**:23150.

67. Liu J, Ludwig B, Liu Y, Zheng Z, Wang F, Tang M, Wang J, Wang J, Pan H, Wang Y: **Scalable dry printing manufacturing to enable long-life and high energy lithium-ion batteries**. *Adv Mater Technol* 2017, **2**:1700106.

68. Kirsch DJ, Lacey SD, Kuang Y, Pastel G, Xie H, Connell JW, Lin Y, Hu L: **Scalable dry processing of binder-free lithium-ion battery electrodes enabled by holey graphene**. *ACS Appl Energy Mater* 2019, **2**:2990–2997.

69. Zhen E, Jiang J, Lv C, Huang X, Xu H, Dou H, Zhang X: **Effects of binder content on low-cost solvent-free electrodes made by dry-spraying manufacturing for lithium-ion batteries**. *J Power Sources* 2021, **515**:230644.

70. Zhang Z, Wu L, Zhou D, Weng W, Yao X: **Flexible sulfide electrolyte thin membrane with ultrahigh ionic conductivity for all-solid-state lithium batteries**. *Nano Lett* 2021, **21**: 5233–5239.

71. Verdier N, Foran G, Lepage D, Prébé A, Aymé-Perrot D, Dollé M: **Challenges in solvent-free methods for manufacturing electrodes and electrolytes for lithium-based batteries**. *Polymers* 2021, **13**:323.

72. Kwon TY, Kim KT, Oh DY, Song YB, Jun S, Jung YS: **Three-dimensional networking binders prepared in situ during wet-slurry process for all-solid-state batteries operating under low external pressure**. *Energy Storage Mater* 2022, **49**: 219–226.

73. Yokota M, Matsunaga T: **Effect of roll press on consolidation and electric/ionic-path formation of electrodes for all-solid-state battery**. *J Power Source Adv* 2021, **12**:100078.

74. Doux J-M, Yang Y, Tan DHS, Nguyen H, Wu EA, Wang X, Banerjee A, Meng YS: **Pressure effects on sulfide electrolytes for all solid-state batteries**. *J Mater Chem A* 2020, **8**: 5049–5055.

75. Koerver R, Aygün I, Leichtweiß T, Dietrich C, Zhang W, Binder JO, Hartmann P, Zeier WG, Janek J: **Capacity fade in solid-state batteries: interphase formation and chemo-mechanical processes in nickel-rich layered oxide cathodes and lithium thiophosphate solid electrolytes**. *Chem Mater* 2017, **29**:5574–5582.

76. Han Y, Jung SH, Kwak H, Jun S, Kwak HH, Lee JH, Hong S-T, Jung YS: **Single- or poly-crystalline Ni-rich layered cathode, sulfide or halide solid electrolyte: which will be the winners for all-solid-state batteries?** *Adv Energy Mater* 2021, **11**: 2100126.